Noninvasive modulation of essential tremor with focused ultrasonic waves

Journal of Neural Engineering

PAPER

Noninvasive modulation of essential tremor with focused ultrasonic waves

Thomas S Riis[1], **Adam J Losser**[1], **Panagiotis Kassavetis**[2], **Paolo Moretti**[2,3,*] **and Jan Kubanek**[1,*]

[1] Department of Biomedical Engineering, University of Utah, Salt Lake City, UT 84112, United States of America
[2] Department of Neurology, University of Utah, Salt Lake City, UT 84132, United States of America
[3] George E. Wahlen, VA, Salt Lake City Health Care System, Salt Lake City, UT 84148, United States of America
[*] Authors to whom any correspondence should be addressed.

E-mail: paolo.moretti@hsc.utah.edu and jan.kubanek@utah.edu

Keywords: ultrasonic neuromodulation, deep brain, thalamus, humans, motor behavior

Supplementary material for this article is available online

OPEN ACCESS

RECEIVED
25 October 2023

REVISED
21 January 2024

ACCEPTED FOR PUBLICATION
9 February 2024

PUBLISHED
27 February 2024

Abstract

Objective: Transcranial focused low-intensity ultrasound has the potential to noninvasively modulate confined regions deep inside the human brain, which could provide a new tool for causal interrogation of circuit function in humans. However, it has been unclear whether the approach is potent enough to modulate behavior. *Approach*: To test this, we applied low-intensity ultrasound to a deep brain thalamic target, the ventral intermediate nucleus, in three patients with essential tremor. *Main results*: Brief, 15 s stimulations of the target at 10% duty cycle with low-intensity ultrasound, repeated less than 30 times over a period of 90 min, nearly abolished tremor (98% and 97% tremor amplitude reduction) in 2 out of 3 patients. The effect was observed within seconds of the stimulation onset and increased with ultrasound exposure time. The effect gradually vanished following the stimulation, suggesting that the stimulation was safe with no harmful long-term consequences detected. *Significance*: This result demonstrates that low-intensity focused ultrasound can robustly modulate deep brain regions in humans with notable effects on overt motor behavior.

1. Introduction

Low-intensity transcranial focused ultrasound has the potential to modulate deep brain circuits in humans entirely noninvasively [1–4]. Ultrasound can be focused through the intact skull and scalp into circumscribed deep brain regions [5, 6]. In addition, arrays of transducers can focus ultrasound into specified brain targets programmatically, without moving the device or the subject [5, 7]. The precise focusing on command opens unique new possibilities to systematically modulate malfunctioning circuits in each individual. This capability is particularly important for patients with mental and neurological disorders for whom the malfunctioning networks and nuclei are poorly understood [8–13].

Effective modulation of neural circuits with low-intensity focused ultrasound has been demonstrated in rodents [14–16]. However, ultrasonic neuromodulation in humans has appeared less effective and robust [17–25]. In particular, low-intensity ultrasound has yet to demonstrate observable changes in overt, motor behavior in humans.

To test this capacity of this emerging technology, we applied low-intensity focused ultrasound to a deep brain thalamic target, the ventral intermediate nucleus (VIM), in subjects with essential tremor. VIM is a motor thalamic nucleus that connects motor cortex with cerebellum and is located with the termination of the dentatorubrothalamic tract, which mediates motor coordination and fine motor control [26]. This target is a primary choice for deep brain stimulation [27–29] and ablative treatments [26] for its implication in tremor motor control, established clinical efficacy, and relatively low risk of mood or cognitive side effects [29]. We hypothesized that ultrasonic modulation of the VIM should reduce the tremor amplitude, just like in previous studies that used deep brain stimulation [27–29], but now entirely non-invasively.

We found that ultrasonic modulation of the VIM can dramatically reduce tremor amplitude, and there were no side effects reported by the subjects.

2. Methods

2.1. Subjects

This study was approved and designated as non-significant risk by the Institutional Review Board of the University of Utah (IRB #00139661). The candidate subjects constituted a pool of essential tremor patients who were not considering ultrasound ablative treatments of the VIM. Patients were informed of the study during a routine appointment at a movement disorder clinic. From this pool, candidates who showed moderate-to-severe tremor and who gave informed consent were included in this study. Following the selection, three patients (male, aged 69 (Subject 1), 79 (Subject 2), 46 (Subject 3)) with moderate-to-severe essential tremor were recruited. Participants abstained from tremor-modulating medication, caffeine, and alcohol at least 24 h prior to the experiment.

2.2. Tremor Measurements

Tremor amplitude was quantified with a hand-worn, MRI-compatible accelerometer (TSD109C2, Biopac Systems). The accelerometer provides three outputs, simultaneously measuring acceleration along the *X*-, *Y*-, and *Z*-axes. The accelerometer was attached with a velcro strap to the distal portion of the subject's palm (figure 1(b)). Analog signals from the accelerometer were digitized and recorded outside of the MRI room (MP150, Biopac Systems). A trigger signal from the ultrasound transducer elements was simultaneously recorded to indicate when in the recordings the transducers were emitting ultrasound.

In addition to accelerometer measurements, a physician administered the Fahn-Tolosa-Marín tremor rating scale [30] approximately 10 min before and after the experiment.

2.3. Task

Subjects laid in a supine position with arms resting at their side. Upon verbal command, subjects raised their arm above their body partially abducted and extended with the elbow at approximately 30 degrees of flexion (figure 1(e), supplementary video 1). Subjects held their arm in this position for 45 s until hearing a verbal command to rest, returning the arm back down by their side. Verbal command was relayed to the subjects through earbuds. White noise was played continuously in the earbuds throughout the experiment to mask potential auditory perception of the ultrasound [31].

During the 45 s trial, ultrasound was turned on at the 15 s mark to acquire a baseline reading of tremor amplitude for the trial. Ultrasound was delivered over the next 15 s. The subjects kept their arm raised for the final 15 s to obtain a measure of post-stimulation tremor amplitude. The behavioral task was repeated over the experimental session with rest time (about 2 min) in between trials and a 15 min break in the middle of the 90 min session. Sham sonications, where no ultrasound was delivered within the trial, were interleaved randomly.

Subjects began the session with three trials without sonication to assess baseline level of tremor. The median of the tremor amplitude across these trials was used as the subject's initial tremor amplitude.

2.4. Signal Analysis

The BIOPAC system digitized the accelerometer signals at 1000 Hz in each dimension along with the trigger out signal of the ultrasound hardware, which indicated when the ultrasound was on. The frequency range measured by the accelerometer extended from DC to 500 Hz, so sampling at 1000 Hz was sufficient. Prior to analyses, all accelerometer recordings were highpass filtered with a cut-off frequency of 1 Hz (1st order Butterworth filter). These signals were analyzed for tremor power amplitude using the following steps [32, 33]: First, we identified the pre- and post- sonication epochs of 10 s in duration using the recorded trigger signal. Only the final 10 s of the pre-sonication and first 10 s of the post-sonication interval were used to eliminate motion artifacts associated with raising and lowering the subject's hand between the active and rest position. The sonication window was taken as the entire 15 s window between onset and offset. The three windows combined form a continuous time interval of trial signals considered in subsequent analyses. Second, signals were bandpass-filtered between 1 and 20 Hz to eliminate potential motion artifacts and frequencies above the tremor range. Third, we integrated the power spectrum of each individual dimension (x, y, z) of the accelerometer signals. And finally, we summed the integrated power spectrum across the three dimensions, thus obtaining the total power of the tremor amplitude [33]. We performed all analyses offline and separately for each condition of pre-sonication, ultrasound-on, and post-sonication.

Tremor dynamics over the entire trial were calculated by binning the data of each epoch into windows of 2.5 s and calculating the power spectrum of each window. Then, we repeated the total tremor power analysis above for each 2.5 s window, integrating the spectrum of the accelerometer signals.

2.5. Ultrasonic System

The ultrasound array system has been described and used previously [7, 34]. Briefly, the hardware consisted of two spherically focused phased arrays mounted to a rigid plastic frame such that they were positioned opposite to each other and separated by a distance of 180 mm. The array elements of both transducers had a surface area of 6 mm × 6 mm, and operated at a fundamental frequency of 650 kHz. Each array had a height of 55 mm and a width of 86 mm,

spanning an area of 47.3 cm^2 (radius of 165 mm; 126 elements; 9 × 14 element grid, inter-element spacing of 0.5 mm).

The transducers were positioned over the left and right sides of the subjects' head and delivered ultrasound through the parietal and temporal bones. The transducers were driven by a programmable system (Vantage256, Verasonics).

2.6. Targeting

Targeting with ultrasound rests on emitting ultrasound from each element such that the wavefronts arrive into the defined target at the same time to create constructive interference. These values were established using the knowledge of the distance from target to the transducer elements and dividing the travel distance by the speed of sound in brain tissue. After calculating these delays, we adjusted their value based on the measured speedup values through the subject's skull as described in previous work [7].

We performed device-to-subject registration to find the target's location relative to the transducers' position. The patients' head was immobilized with a standard radiological thermoplastic mask (Aquaplast RT Open Eye and Mouth Slimline U-Frame; QFix, Avondale, PA). To coregister the transducer with subject-specific brain anatomy, we took a standard anatomical T1-weighted image of the subject and the transducers (figure 1(a)). The transducer arrays' position was registered to the subject's MRI using fiducial markers.

The position of the VIM was identified by first finding the position of the anterior commissure (AC) and posterior commissure (PC) of the subject's brain using an automatic detection algorithm [35] (figure 1(a)). We set the focal point to a standard 15 mm lateral and 6 mm anterior to the posterior commissure along the AC-PC line [36]. We stimulated the VIM contralateral to the tremor-dominant hand carrying the accelerometer. We focused the ultrasound from the phased arrays into this location after applying a correction for the skull attenuation and dephasing [7]. The arrays produce an intensity field with lateral × elevational × axial dimensions of 2.4 mm × 3.6 mm × 20.4 mm (y, z, and x dimensions of the Montreal Neurological Institute coordinate system). The total field volume of 0.142 cm^3 was equivalent to a sphere with a radius of 3.24 mm [7].

2.7. Deep Brain Stimulation

The ultrasound was delivered into the target (VIM of the thalamus) in 10 ms pulses (650 kHz, 0.72 MPa peak pressure following correction for the skull) every 100 ms over the 15 s total sonication duration. The device automatically calculates the attenuation of the ultrasound by the skull, scalp, and hair, and compensates for these obstacles prior to the stimulation [7, 37]. This correction circumvents the need for hair shaving, so the participants' hair was not shaved. The frequency of 650 kHz was chosen as a compromise between higher frequencies that provide sharper focus and lower frequencies that are less attenuated by the skull [5]. The pressure and pulsing parameters were chosen to be similar to previous ultrasound neuromodulation studies [38–40] while staying close to the FDA 510(k) Track 3 guidelines [41]: $I_{SPPA} = P^2/(2\rho c) = 16.12\,\mathrm{W\,cm^{-2}}$ and $I_{SPTA} = DC * I_{SPPA} = 1.612\,\mathrm{W\,cm^{-2}}$, where P is pressure, ρ is the density of brain tissue, c is the speed of sound in the brain, and DC is the duty cycle over the 15 s sonication window.

3. Results

We have developed an ultrasonic neuromodulation array that enables effective and safe modulation of deep brain circuits in humans [7, 37]. Using this device, we now aim to address a key question in the ultrasonic neuromodulation field, i.e., whether low-intensity transcranial focused ultrasound can induce observable changes in overt, motor behavior of human subjects.

For this purpose, we capitalized on the well-understood neural substrates associated with essential tremor, the VIM. Modulation of the VIM with deep brain stimulation is known to substantially reduce tremor amplitude [27, 28]. If remotely applied ultrasound also exerts neuromodulatory effects on this deep brain structure, we would predict a disruption to the propagating tremor signal and a subsequent reduction in tremor amplitude.

Figure 1 shows the experimental setup, which consists of the ultrasonic device (figure 1(a)) and an accelerometer that continuously measures tremor amplitude over the tremor-dominant hand (figure 1(b)). We harnessed the unique opportunity to apply the approach in three subjects with essential tremor (University of Utah). In these subjects, we applied low-intensity, low-frequency ultrasound to the VIM for 15 s each trial at 10% duty cycle and an average of 23 trials per subject over a period of 90 min (see Methods).

This stimulation regimen led to a substantial reduction in the measured tremor amplitude in two of the three subjects (figures 1(c) and 2). Compared to the baseline tremor level, the average post-sonication tremor amplitude in the final 10 trials of each session was 1.9 ± 2.4%, 125 ± 98.1%, and 2.9 ± 2.1% (mean ± s.d.) for subjects one, two and three, respectively.

The difference between the tremor amplitude in these last 10 trials compared with the baseline amplitude was significant in subjects one ($t_{12} = 23.04$, $p = 2.6 \times 10^{-11}$, two-sample t-test) and three ($t_{12} = 6.1$,

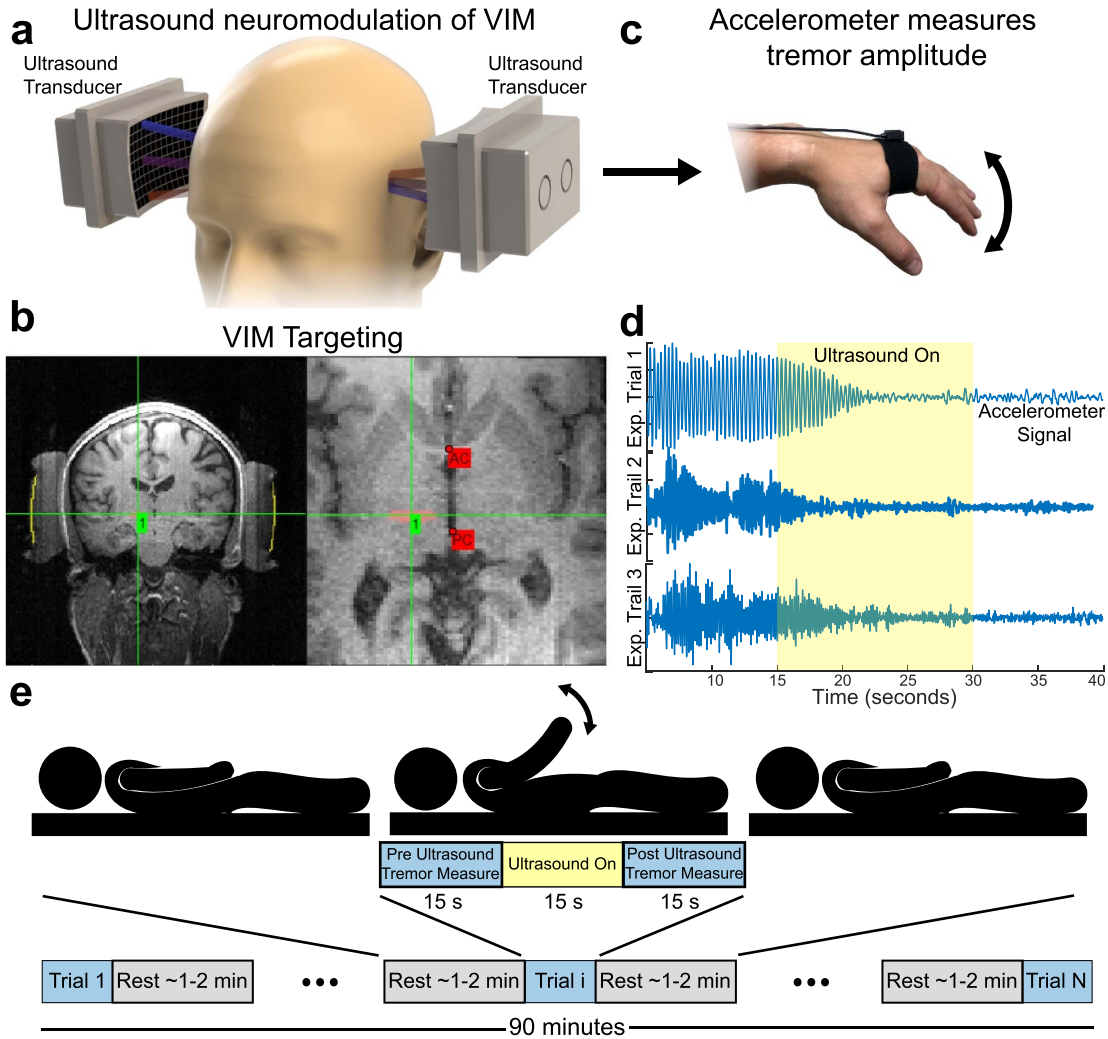

Figure 1. Apparatus for noninvasive deep brain modulation of essential tremor. (a) Ultrasonic neuromodulation device used in this experiment [7] consisting of two 126 element phased arrays covering the left and ride sides of head. (b) Example operation of the device targeting the ventral intermediate nucleus (VIM) of the thalamus (green crosshair) based on anterior commissure (AC) and posterior commissure (PC) (red) coordinates (Methods). The pink ellipse under the green crosshairs shows the half-maximum intensity field at target, with dimensions of 2.4 mm × 3.6 mm × 20.4 mm (y, z, and x; Montreal Neurological Institute coordinate system) [7]. (c) An accelerometer fixed to the participant's hand measures tremor amplitude during the experiment. (d) Example accelerometer signals (normalized, bandpassed 1–20 Hz). The three traces exemplify effects in subjects 1, 2 and 3, respectively. (e) In each trial, the subjects were asked to raise their hand above their body to capture the subject's tremor; the ultrasound was applied 15 s following this instruction, for 15 s. Subjects held their arm in the raised position 15 s following the offset of the ultrasound, and subsequently rested with arms at their side. Subjects rested for a period of 1–2 min between trials and this process recurred over the 90 min experiment.

$p = 5.3 \times 10^{-5}$, two-sample t-test). There was no significant effect in subject two ($t_{12} = -0.46$, $p = 0.66$, two-sample t-test).

We observed a progressive decrease in the total trial tremor amplitude in all three subjects over the course of the experiment (figure 3). The tremor amplitude decreased with the number of stimulation epochs received (Subject 1: $y = -0.028x + 0.77$, $p = 0.000083$, $R^2 = 0.50$; Subject 2: $y = -0.026x + 1.67$, $p = 0.18$, $R^2 = 0.07$; Subject 3: $y = -0.029x + 0.42$, $p = 0.004$, $R^2 = 0.40$). The decrease in tremor over time across all subjects was significant (significance of slope: $t_2 = -32.2$, $p = 0.00097$, two-tailed t-test). Analysis of covariance showed a significant dependence of tremor amplitude on the sonication number (ANCOVA: $F_{1,64} = 10.5$, $p = 0.0018$). We found no significant interaction between sonication number and subject ($F_{2,64} = 0.03$, $p = 0.967$), indicating a consistent effect across the subjects.

We assessed these effects also on a trial-wise basis (figure 4, supplementary movie 1), and also evaluated effects during sham stimulation. Compared to the pre-stimulation tremor amplitude, post-stimulation amplitude was reduced by 65.85 ± 43.13% (mean ± s.d.) for subject 1, reduced by 91.28 ± 7.88% for subject 3, and increased by 66.06 ± 130% for subject 2. Figure 4(b) shows tremor power decreases within seconds of the ultrasound onset for

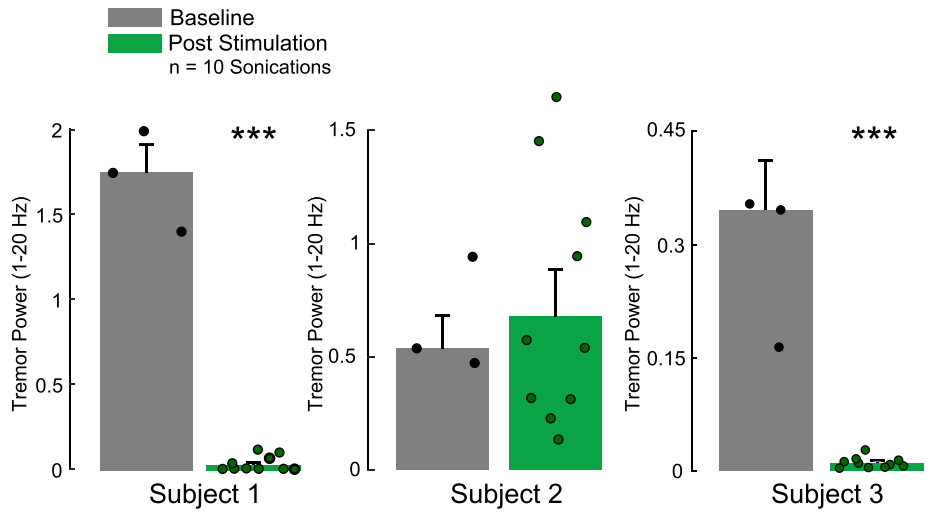

Figure 2. Low-intensity transcranial focused ultrasound applied to the VIM nucleus of the thalamus suppresses tremor amplitude. Mean±s.e.m. tremor amplitude in the post-sonication window averaged across the final ten stimulation trials of each session relative to pre-treatment baseline measures, separately for each subject. The difference was assessed using a two-sample t-test: $^{***}p < 0.001$.

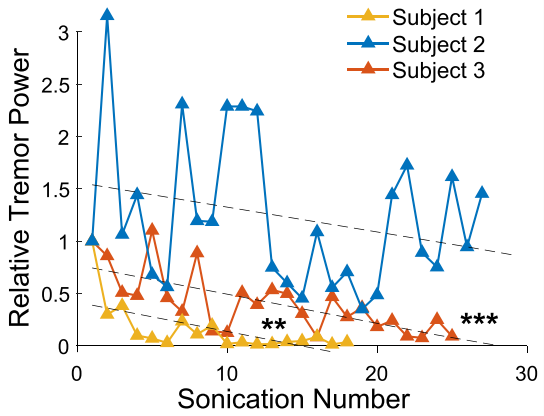

Figure 3. Durable decrease of tremor in response to repeated stimulation. Total tremor amplitude computed over each stimulation repetition (i.e. each trial: pre-sonication window, sonication window, post-sonication window (see Methods)) as a function of the number of each stimulation repetition. The data were normalized to baseline, so that each trace starts at the value of 1. The dashed lines shows linear fits to the data. Stars denote the cases in which the slope was significant ($^{***}p < 0.001$; $^{**}p < 0.01$).

subject 1 and subject 3, while subject 2 showed a moderate increase in average tremor power following ultrasound stimulation. Sham stimulations, in which no ultrasound was emitted, were randomly interleaved with the verum stimulations. There was a significant difference between the verum and sham tremor effects in both subjects that exhibited the effect (i.e. subjects 1 and 3: $t_{18} = 2.40$, $p = 0.027$ and $t_{31} = 3.51$, $p = 0.0014$; two-sample t-test).

We found that repeated stimulation of the VIM with focused ultrasound was well tolerated. The tremor amplitude returned to pre-stimulation state within about 20 minutes following the last stimulation, as judged by neurological examination (Methods). No adverse events were noted and subjects did not note any side effects in the 24 h post experiment they were monitored for.

4. Discussion

We found that remotely applied, low-intensity ultrasound modulation of a deep brain nucleus involved in essential tremor can substantially decrease tremor amplitude. In two of three subjects, there was a nearly complete elimination of the tremor, with amplitude reductions greater than 95%. Therefore, low-intensity ultrasound has the capacity to modulate overt, motor behavior in humans.

Two principal effects were observed—transient, in which the tremor amplitude was reduced within seconds of stimulation onsets (figure 1(d), figure 4(b))—and cumulative, in which the tremor amplitude gradually decreased over the course of the individual ultrasound doses (figure 3). Both effects have been described in ultrasonic neuromodulation literature and they commonly depend on the total ultrasound exposure. Specifically, brief stimuli, on the order of several seconds (our stimulus lasted 15 seconds in each trial), induce neuromodulation effects on the order of seconds [38, 42]. On the other hand, longer stimuli commonly produce durable changes to functional connectivity within the target circuits [43–46]. Beyond stimulus duration, neuromodulation effectiveness is a function of the ultrasound frequency, pressure, pulse repetition frequency, and duty cycle [31, 39]. The frequency used in this study (650 kHz), while higher than previous neuromodulation applications in humans

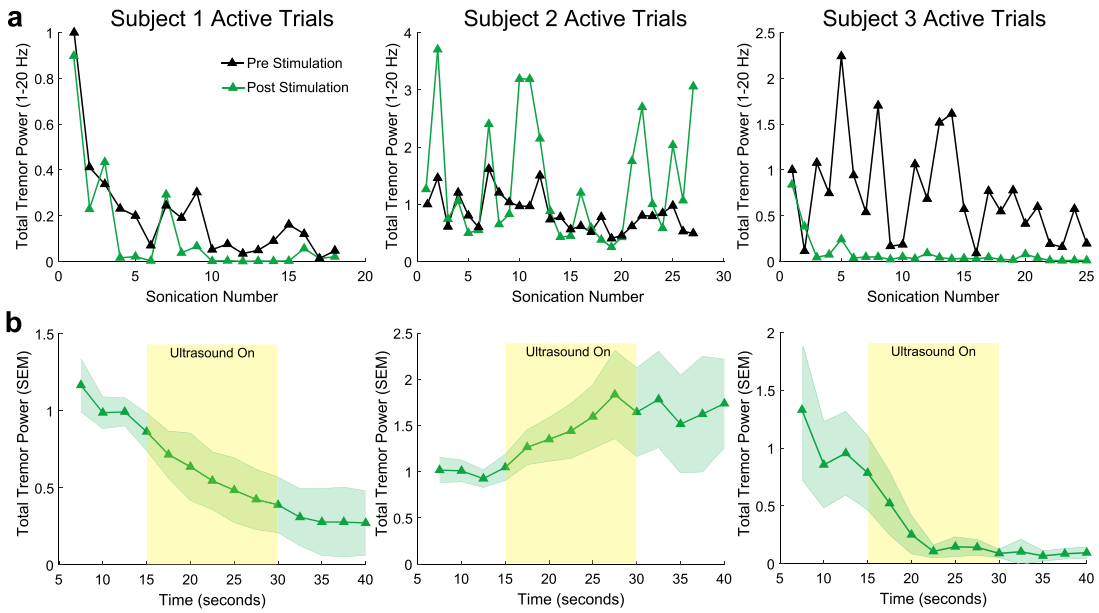

Figure 4. Tremor dynamics in response to repeated stimulation. (a) Pre and post stimulation tremor total power for each subject across all active trials. (b) Average and standard error (SEM) tremor total power dynamics throughout the trial. The yellow rectangle indicates the ultrasound delivery window.

(<500 kHz) [47], was chosen as a tradeoff between focal volume and the ultrasound attenuation by the human head. The frequency was also chosen to be compatible with an existing transcranial-focused ultrasound surgical device [5]. Further, the skull correction method used here [37] enabled a compensation for the increased attenuation of this relatively high frequency. Previous studies validated the neuromodulatory efficacy of this parameter, being appropriate to modulate fMRI blood oxygenation level-dependent activity at target and to induce mood changes in subjects with major depressive disorder [7, 34]. The pulse repetition frequency and duty cycle were chosen to maximize acoustic intensity and acoustic duration to enhance efficacy [48] while minimizing heating. We chose a pulse duration of 10 ms as a lower bound on the duration needed to elicit neuromodulatory effects at the emitted pressure [31, 38–40], and set the pulse repetition period such as to comply with FDA 510(k) Track 3 guidelines [41] over the duration of the experiment. Neuromodulatory effectiveness may also be influenced by temperature increases or enhanced acoustic radiation forces induced by this particular setup. For these parameters, we estimated maximal temperature increase using the bioheat equation, $\Delta T = \frac{2\alpha I \Delta t}{\rho C} = 0.53°\mathrm{C}$, where α is the absorption of brain tissue ($0.06f = 0.06(0.65) = 3.9\ \mathrm{m}^{-1}$), C is the specific heat of the brain ($3630\ \mathrm{J\,kg^{-1}\,K^{-1}}$), ρ is the density of brain tissue ($1030\ \mathrm{kg\ m^{-3}}$), I is the spatial peak temporal average intensity (I_{SPTA} in brain tissue ($1.612\ \mathrm{W\,cm^{-2}}$), and Δt is the sonication duration (15 s) [49]. The equation does not include heat conduction and convection and therefore provides an upper bound estimate on the temperature rise. Acoustic radiation force is also considered one of the physical mechanisms underlying effective neuromodulation. The two opposing transducers used in this study create a standing wave at the focus that generates a significantly larger acoustic radiation forces than single element transducers [50], which may enhance the effectiveness of the neuromodulation [4, 51].

In this initial study for this particular purpose, we have placed emphasis on safety, delivering into the target a relatively modest amount of ultrasound energy. The stimulation was safe and well tolerated by all three subjects with no side effects noted. With the transducers centered over the thalamus, we chose to avoid active sham with unfocused or off-target stimulation as performed previously [7] to mitigate the risks of stimulating this highly interconnected area or the surrounding deep brain structures.

The modest ultrasound exposure used in this study led to relatively short-lived effects, on the order of dozens of minutes. Although this effect duration is likely not sufficient for therapeutic applications, it is well suited for systematic dissection of neural circuits in humans. In this approach, the individual candidate regions can be perturbed systematically, one by one, until identifying the targets that modulate a given sign, symptom, or behavior most strongly. This iterative approach is conceptually analogous to the pre-ablation surgical planning used in high-intensity focused ultrasound treatments for essential tremor, which induces a significant temperature increase (>10 °C) to inhibit target areas temporarily [5]. The neuromodulatory approach used here delivered orders of magnitude lower ultrasound intensity [5].

At this low level, harmful heating of the target or the skull would not be expected [52], thus providing a safer alternative for noninvasive manipulations of localized brain regions in humans. This neuromodulatory approach has a unique potential for causal brain mapping, identifying the neural circuits that are crucially involved in—as opposed to just encoding—a given sign, symptom, or behavior. This information could be used for diagnostic and basic science purposes, as well as translational purposes such as guidance of deep brain stimulation implants.

Using the same device, we recently delivered a substantial amount of ultrasound energy, for a total duration of 50 min of stimulation, into the subgenual cingulate cortex of a subject with major depression [34]. Following this exposure, we found that the subject's depression symptoms resolved within the first day and the beneficial effects lasted for several weeks [34]. Therefore, there is evidence that the approach reported here, when delivering substantially more ultrasound energy, could also provide therapeutic benefits to patients. These durable effects provide a unique opportunity for noninvasive reset of the malfunctioning circuits in each individual.

There were notable effects in two of the three subjects. The lack of an effect in one of the subjects—or just a trend toward a decrease over time—is likely caused by the targeting difficulties of precise registration and phase aberrations caused by delivering ultrasound through the human skull. The skull can strongly aberrate the beam, to the point that the delivered focal coordinate can differ markedly from the intended coordinate [37]. The VIM nucleus is approximately $4 \times 4 \times 6$ mm in size (x, y, z) [53], making it a difficult to match the size of the ultrasound focus used in this experiment ($2.4 \times 3.6 \times 20.4$ mm; y, z, and x dimensions of the MNI coordinate system). Further, during treatment planning, we noticed that the transducers were set at a sharper angle to the skull in the coronal plane, which may have accentuated the refraction of the ultrasound beam. Given these targeting issues, it is critical to develop MRI-based approaches, such as MRI ARFI [54, 55], to directly visualize and validate the ultrasound targeting. The availability of such guidance tools is expected to increase the uniformity of outcomes associated with this highly precise tool. Future studies would additionally benefit from an active control to improve comparison with sham and test the target specificity necessary to reduce tremor. Stimulating the ipsilateral VIM or lateral ventricles could provide an off-target stimulation comparison while minimizing the risk of ultrasound exposure to these deep brain areas. In the absence of an active sham, future studies may improve the white noise auditory masking used in this study by overlaying pure tones or sham audio of ultrasound pulses over white noise timed to the ultrasound stimulation parameters [56]. Nevertheless, the tremor reduction reported in this study outlived the ultrasound stimulation window, which suggests that the effects were not due to an auditory perception of the ultrasound stimulus or other indirect effects (figure 4).

The finding that low-intensity ultrasound has the capacity to modulate overt, motor behavior in humans following modulation of a deep brain nucleus encourages the deployment of this approach in precision diagnoses and treatments of the neural circuits involved in mental and neurological disorders, as well as for dissecting the function of neural circuits in humans.

Data availability statement

The data cannot be made publicly available upon publication because they contain commercially sensitive information. The data that support the findings of this study are available upon reasonable request from the authors.

Acknowledgments

This work was supported by the NIH Grants R00NS100986, RF1NS128569, and S10OD026788, the University of Utah College of Engineering Seed grant, and the University of Utah Ascender grant.

ORCID iDs

Thomas S Riis https://orcid.org/0000-0003-0719-5114
Jan Kubanek https://orcid.org/0000-0003-0527-5559

References

[1] Naor O, Krupa S and Shoham S 2016 Ultrasonic neuromodulation *J. Neural Eng.* **13** 031003
[2] Kubanek J 2018 Neuromodulation with transcranial focused ultrasound *Neurosurg. Focus* **44** E14
[3] Tyler W J, Lani S W and Hwang G M 2018 Ultrasonic modulation of neural circuit activity *Curr. Opin. Neurobiol.* **50** 222–31
[4] Blackmore J, Shrivastava S, Sallet J, Butler C R and Cleveland R O 2019 Ultrasound neuromodulation: a review of results, mechanisms and safety *Ultrasound Med. Biol.* **45** 1509–36
[5] Ghanouni P, Pauly K B, Elias W J, Henderson J, Sheehan J, Monteith S and Wintermark M 2015 Transcranial MRI-guided focused ultrasound: a review of the technologic and neurologic applications *Am. J. Roentgenol.* **205** 150–9
[6] Harary M, Essayed W I, Valdes P A, McDannold N and Cosgrove G R 2018 Volumetric analysis of magnetic resonance–guided focused ultrasound thalamotomy lesions *Neurosurg. Focus* **44** E6
[7] Riis T, Feldman D, Losser A, Mickey B and Kubanek J 2023 Device for multifocal delivery of ultrasound into deep brain regions in humans *IEEE Trans. Biomed. Eng.* **71** 660–8

[8] Price J L and Drevets W C 2012 Neural circuits underlying the pathophysiology of mood disorders *Trends Cogn. Sci.* **16** 61–71
[9] Widge A S and Dougherty D D 2015 Deep brain stimulation for treatment-refractory mood and obsessive-compulsive disorders *Curr. Behav. Neurosci. Rep.* **2** 187–97
[10] Braun U, Schaefer A, Betzel R F, Tost H, Meyer-Lindenberg A and Bassett D S 2018 From maps to multi-dimensional network mechanisms of mental disorders *Neuron* **97** 14–31
[11] Kuhn J, Gaebel W, Klosterkoetter J and Woopen C 2009 Deep brain stimulation as a new therapeutic approach in therapy-resistant mental disorders: ethical aspects of investigational treatment *Eur. Arch. Psychiatry Clin. Neurosci.* **259** 135–41
[12] Dandekar M, Fenoy A, Carvalho A, Soares J and Quevedo J 2018 Deep brain stimulation for treatment-resistant depression: an integrative review of preclinical and clinical findings and translational implications *Mol. Psychiatry* **23** 1094–112
[13] Scangos K W, Makhoul G S, Sugrue L P, Chang E F and Krystal A D 2021 State-dependent responses to intracranial brain stimulation in a patient with depression *Nat. Med.* **27** 229–31
[14] Tufail Y, Matyushov A, Baldwin N, Tauchmann M L, Georges J, Yoshihiro A, Tillery S I H and Tyler W J 2010 Transcranial pulsed ultrasound stimulates intact brain circuits *Neuron* **66** 681–94
[15] Ye P P, Brown J R and Pauly K B 2016 Frequency dependence of ultrasound neurostimulation in the mouse brain *Ultrasound Med. Biol.* **42** 1512–30
[16] Lee W, Croce P, Margolin R W, Cammalleri A, Yoon K and Yoo S-S 2018 Transcranial focused ultrasound stimulation of motor cortical areas in freely-moving awake rats *BMC Neurosci.* **19** 1–14
[17] Legon W, Sato T F, Opitz A, Mueller J, Barbour A, Williams A and Tyler W J 2014 Transcranial focused ultrasound modulates the activity of primary somatosensory cortex in humans *Nat. Neurosci.* **17** 322–9
[18] Lee W, Kim H, Jung Y, Song I-U, Chung Y A and Yoo S-S 2015 Image-guided transcranial focused ultrasound stimulates human primary somatosensory cortex *Sci. Rep.* **5** 8743
[19] Fomenko A *et al* 2020 Systematic examination of low-intensity ultrasound parameters on human motor cortex excitability and behavior *eLife* **9** e54497
[20] Legon W, Ai L, Bansal P and Mueller J K 2018 Neuromodulation with single-element transcranial focused ultrasound in human thalamus *Hum. Brain Mapp.* **39** 1995–2006
[21] Lee W, Kim H-C, Jung Y, Chung Y A, Song I-U, Lee J-H and Yoo S-S 2016 Transcranial focused ultrasound stimulation of human primary visual cortex *Sci. Rep.* **6** 34026
[22] Legon W, Bansal P, Tyshynsky R, Ai L and Mueller J K 2018 Transcranial focused ultrasound neuromodulation of the human primary motor cortex *Sci. Rep.* **8** 1–14
[23] Ai L, Bansal P, Mueller J K and Legon W 2018 Effects of transcranial focused ultrasound on human primary motor cortex using 7T fMRI: a pilot study *BMC Neurosci.* **19** 1–10
[24] Sanguinetti J L, Hameroff S, Smith E E, Sato T, Daft C M, Tyler W J and Allen J J 2020 Transcranial focused ultrasound to the right prefrontal cortex improves mood and alters functional connectivity in humans *Front. Hum. Neurosci.* **14** 52
[25] Badran B W *et al* 2020 Sonication of the anterior thalamus with mri-guided transcranial focused ultrasound (tFUS) alters pain thresholds in healthy adults: a double-blind, sham-controlled study *Brain Stimul.* **13** 1805–12
[26] Dallapiazza R F, Lee D J, De Vloo P, Fomenko A, Hamani C, Hodaie M, Kalia S K, Fasano A and Lozano A M 2019 Outcomes from stereotactic surgery for essential tremor *J. Neurol. Neurosurg. Psychiatry* **90** 474–82
[27] Perlmutter J S and Mink J W 2006 Deep brain stimulation *Annu. Rev. Neurosci.* **29** 229–57
[28] Mitchell K T *et al* 2019 Benefits and risks of unilateral and bilateral ventral intermediate nucleus deep brain stimulation for axial essential tremor symptoms *Parkinsonism Relat. Disorders* **60** 126–32
[29] Iorio-Morin C, Fomenko A and Kalia S K 2020 Deep-brain stimulation for essential tremor and other tremor syndromes: a narrative review of current targets and clinical outcomes *Brain Sci.* **10** 925
[30] Fahn S, Tolosa E and Marin C 1993 Clinical rating scale for tremor *Parkinson's Disease and Movement Disorders* 2nd edn (Urban & Schwarzenberg) pp 225–34
[31] Zeng K, Darmani G, Fomenko A, Xia X, Tran S, Nankoo J-F, Oghli Y S, Wang Y, Lozano A M and Chen R 2022 Induction of human motor cortex plasticity by theta burst transcranial ultrasound stimulation *Ann. Neurol.* **91** 238–52
[32] Gauthier-Lafreniere E, Aljassar M, Rymar V V, Milton J and Sadikot A F 2022 A standardized accelerometry method for characterizing tremor: application and validation in an ageing population with postural and action tremor *Front. Neuroinform.* **16** 1–14
[33] Elble R J and McNames J 2016 Using portable transducers to measure tremor severity *Tremor Other Hyperkinetic Mov.* **6** 375
[34] Riis T, Feldman D, Lily V, Brown J, Solzbacher D, Kubanek J and Mickey B 2023 Durable effects of deep brain ultrasonic neuromodulation on major depression: a case report *J. Med. Case Rep.* **17** 449
[35] Ardekani B A and Bachman A H 2009 Model-based automatic detection of the anterior and posterior commissures on MRI scans *NeuroImage* **46** 677–82
[36] Chang W S, Jung H H, Kweon E J, Zadicario E, Rachmilevitch I and Chang J W 2015 Unilateral magnetic resonance guided focused ultrasound thalamotomy for essential tremor: practices and clinicoradiological outcomes *J. Neurol. Neurosurg. Psychiatry* **86** 257–64
[37] Riis T, Mickey B, Feldman D and Kubanek J 2024 Controlled noninvasive modulation of deep brain regions in humans *Comms. Eng.* **3** 13
[38] Kubanek J, Brown J, Ye P, Pauly K B, Moore T and Newsome W 2020 Remote, brain region–specific control of choice behavior with ultrasonic waves *Sci. Adv.* **6** eaaz4193
[39] Riis T and Kubanek J 2021 Effective ultrasonic stimulation in human peripheral nervous system *IEEE Trans. Biomed. Eng.* **69** 15–22
[40] Folloni D, Verhagen L, Mars R B, Fouragnan E, Constans C, Aubry J-F, Rushworth M F and Sallet J 2019 Manipulation of subcortical and deep cortical activity in the primate brain using transcranial focused ultrasound stimulation *Neuron* **101** 1109–16
[41] FDA 2019 Marketing clearance of diagnostic ultrasound systems and transducers *Food and Drug Administration* FDA-2017-D-5372
[42] Webb T D, Wilson M G, Odéen H and Kubanek J 2022 Remus: system for remote deep brain interventions *iScience* **25** 105251
[43] Webb T D, Wilson M G, Odéen H and Kubanek J 2023 Sustained modulation of primate deep brain circuits with focused ultrasonic waves *Brain Stimul.* **16** 798–805
[44] Verhagen L *et al* 2019 Offline impact of transcranial focused ultrasound on cortical activation in primates *eLife* **8** e40541
[45] Fouragnan E F *et al* 2019 The macaque anterior cingulate cortex translates counterfactual choice value into actual behavioral change *Nat. Neurosci.* **22** 797–808
[46] Khalighinejad N, Bongioanni A, Verhagen L, Folloni D, Attali D, Aubry J-F, Sallet J and Rushworth M F 2020 A basal forebrain-cingulate circuit in macaques decides it is time to act *Neuron* **105** 370–84
[47] Sarica C *et al* 2022 Human studies of transcranial ultrasound neuromodulation: a systematic review of effectiveness and safety *Brain Stimul.* **15** 737–46
[48] King R L, Brown J R, Newsome W T and Pauly K B 2013 Effective parameters for ultrasound-induced *in vivo* neurostimulation *Ultrasound Med. Biol.* **39** 312–31

[49] Yu K, Niu X, Krook-Magnuson E and He B 2021 Intrinsic functional neuron-type selectivity of transcranial focused ultrasound neuromodulation *Nat. Commun.* **12** 2519
[50] Kim Y H, Kang K C, Kim J N, Pai C N, Zhang Y, Ghanouni P, Park K K, Firouzi K and Khuri-Yakub B T 2022 Patterned interference radiation force for transcranial neuromodulation *Ultrasound Med. Biol.* **48** 497–511
[51] Menz M D, Ye P, Firouzi K, Nikoozadeh A, Pauly K B, Khuri-Yakub P and Baccus S A 2019 Radiation force as a physical mechanism for ultrasonic neurostimulation of the ex vivo retina *J. Neurosci.* **39** 6251–64
[52] Pulkkinen A, Huang Y, Song J and Hynynen K 2011 Simulations and measurements of transcranial low-frequency ultrasound therapy: skull-base heating and effective area of treatment *Phys. Med. Biol.* **56** 4661–83
[53] Sammartino F, Krishna V, King N K K, Lozano A M, Schwartz M L, Huang Y and Hodaie M 2016 Tractography-based ventral intermediate nucleus targeting: novel methodology and intraoperative validation *Mov. Disorders* **31** 1217–25
[54] Kaye E A, Chen J and Pauly K B 2011 Rapid MR-ARFI method for focal spot localization during focused ultrasound therapy *Magn. Reson. Med.* **65** 738–43
[55] Phipps M A, Jonathan S V, Yang P-F, Chaplin V, Chen L M, Grissom W A and Caskey C F 2019 Considerations for ultrasound exposure during transcranial mr acoustic radiation force imaging *Sci. Rep.* **9** 1–11
[56] Braun V, Blackmore J, Cleveland R O and Butler C R 2020 Transcranial ultrasound stimulation in humans is associated with an auditory confound that can be effectively masked *Brain Stimul.* **13** 1527–34